History-dependent effects in subcycle-waveform strong-field ionization

M. Kolesik,[1,2] J. M. Brown,[1] J. V. Moloney,[1,3] and D. Faccio[1,4]
[1]*College of Optical Sciences, University of Arizona, Tucson Arizona, USA*
[2]*Constantine the Philosopher University, Nitra, Slovakia*
[3]*Arizona Center for Mathematical Sciences, University of Arizona, Tucson Arizona, USA*
[4]*School of Engineering and Physical Sciences, SUPA, Heriot-Watt University, Edinburgh EH14 4AS, United Kingdom*
(Received 5 January 2014; published 15 September 2014)

Recent developments in laser sources allow one to shape the precise electric-field waveform oscillation at the subcycle level. These waveforms may then be used to drive and control ultrafast nonlinear phenomena at the attosecond timescale. By utilizing numerical solutions of time-dependent Schrödinger equations and exact solutions of a simple quantum-mechanical system, we show that an atom driven by such sources exhibit coherent history-dependent effects. These manifest themselves in "macroscopic" quantities such as the yield in multicolor, strong-field ionization. We argue that weakly bound, metastable electronic states may enable the dependence on the system history even in long-duration, relatively weak driving waveforms.

DOI: 10.1103/PhysRevA.90.033414 PACS number(s): 32.80.Rm, 32.80.Qk, 42.65.−k

Introduction. Modern laser pulses are currently the shortest man-made events, with time durations reaching into the sub-100 as regime [1]. Combined with high intensities, these pulses enable the study of light-matter interaction and the observation of electron dynamics on unprecedented timescales. Examples are the measurement of time delays in electron ionization [2], direct observation [3,4] and control [5] of electron tunneling, and real-time visualization of valence electron motion [6]. Although most of these studies are performed in gaseous media, similar dynamics in addition to novel attosecond scale phenomena are being unveiled also in solid-state media [7,8]. These discoveries are driven by the development of laser sources that allow one to control the laser pulse shapes with extreme precision. Initially, this control was limited to the envelope of pulses reaching down to the few-cycle or even single-cycle regime but recent advances involve full tailoring of the actual electric field. Full Fourier synthesis of arbitrarily shaped, periodic electric-field waveforms may be efficiently obtained by combining a set of discrete frequencies, e.g., the Raman-shifted lines or the first several harmonics obtained from a nanosecond pump laser pulse [9–13]. Similar techniques may be applied also with ultrashort pulses for high-harmonic generation [14,15] and the expectation is that subcycle waveform control will open new opportunities for strong-field physics [14].

Particular attention in this context is given to the ionization dynamics in the presence of a strong pulsed electric field because these play such an important role in processes such as ultrashort laser pulse filamentation and frequency conversion to both the soft-x-ray and THz regimes. For a fully resolved (in space and time) simulation of light-matter interaction with optical pulses, *ab initio* methods based on the solution of the underlying quantum problem are too expensive. Therefore, the standard approach to modeling and interpreting atom ionization physics is based on the Keldysh theory [16] and its improvements, such as the Perelomov, Popov, and Terentév (PPT) model [17,18], which gives an estimate of the ionization rate. Regardless of the details of the specific formula that is adopted, the common feature is that the process is treated as effectively instantaneous, and is implemented in a simulation as a function of the instantaneous electric field $E(t)$ or cycle-averaged intensity of the light, $I(t)$. It is therefore insensitive to the previous history of the system.

In this work we unveil the subfemtosecond dynamics of light-matter interaction and show that ionization is not an instantaneous process and, on the contrary, exhibits a marked dependence on history.

Surprisingly, only modest intensities are needed, and the driving pulse does not need to be short. In fact, the effect can accumulate in long-duration waveforms and can therefore become very strong. This conclusion is supported by numerically solving the time-dependent Schrödinger equation (TDSE). Moreover, we also employ an exactly solvable Dirac-δ atom model [19] that allows one to capture the light interaction with the atom and reveals the same effects observed with the full TDSE. The history-dependent effects described here imply that the plasma densities will differ and depend on the specific subcycle shape of the laser pulse waveforms as a result of the attosecond-scale ionization dynamics that are not captured by rate-based ionization formulas. In order to highlight this, we compare two specific waveforms that deliver identical plasma densities in such models but differ significantly when simulated by using both the TDSE and the solvable Dirac-δ model. Of course, that fact alone that ionization depends on the temporal structure of the driving field is not new. For example, Refs. [20,21] study the effects induced by chirp. In particular, Ref. [21] utilized very high frequencies and rather extreme chirps. Here we reveal the history dependence for long-duration wave trains of optical-frequency fields. Moreover, we work in a regime characterized by significantly lower intensities when per-cycle ionization yield remains very low, yet the effect continues to accumulate over long timescales. In Ref. [20], the role of the precise wave shape was demonstrated in the photoelectron energy spectra. It was explained by the standard dynamics of free electrons in the time-dependent external field in which the ion potential plays no role. The mechanism revealed in this work is different in that it requires the presence of both the optical field and the interaction with the atom or ion. Moreover, the differences in ionization yield that we obtain in different driving waveforms are orders of

magnitude larger than in Ref. [20] because they grow with the duration of the pulse. We show that these features are intimately connected to the dynamics of the "to-be-ionized" electron wave packet still weakly interacting with the atomic potential.

Ionization models in spatially resolved simulations. The ionization model commonly used in numerical simulations of light-matter interactions with ultrashort optical pulses is based on the notion of the ionization rate, $W(E(t))$, which specifies the number of atoms ionized per unit of time in a field of strength E. In this approach, the history of the system exposed to the time-dependent electric field of the optical pulse is irrelevant. The rate of free-electron production only depends on the instantaneous value of the electric field $E(t)$ or, alternatively, on the cycle-averaged intensity $I(t)$. An estimate of the rate W is usually obtained from, e.g., the PPT theory and is often parametrized in the form of an effective power law [22]. Alternatively, a tabulation of W can be used. Irrespective of the actual implementation, the important feature present in virtually all current simulations is that the ionization rate does not depend on the history of the system.

In the regime of weak ionization, the survival probability for an atom to remain not ionized can be calculated as $p(t) = 1 - \int_{-\infty}^{t} W(E(\tau))d\tau$. In what follows we utilize this formulation to illustrate the behavior in the standard ionization model and then compare it to approximation-free quantum calculations.

Time-dependent Schrödinger equation simulations. Our main tool to detect the quantum history-dependent effects is the time-domain three-dimensional (3D) Schrödinger equation solved numerically for a single-active-electron atom model,

$$i\,\partial_t \psi\,(\rho,z,t) = -\tfrac{1}{2}\Delta\psi + V\,(\rho,z)\,\psi + F\,(t)\,z\psi, \qquad (1)$$

with a Coulomb potential V and a time-dependent field strength $F(t)$, which represents the electric field of an optical pulse. The computational domain is endowed with perfectly matched layer (PML) transparent boundary conditions to absorb the outgoing component of the field-driven wave function. The observable of interest is the norm of the wave function, $|\langle\psi(t)|\psi(t)\rangle|^2$, with its decay interpreted as a measure of ionization [23].

Exactly solvable, one-dimensional quantum system. As an alternative free of any possible numerical issues, we also utilize an exactly solvable quantum system. This is a well known, one-dimensional model with the Dirac δ function in the role of the atomic potential:

$$i\,\partial_t \psi\,(z,t) = -\tfrac{1}{2}\Delta\psi - \delta\,(z)\,\psi + F\,(t)\,z\psi. \qquad (2)$$

The spectrum of this system consists of a single bound (ground) state plus a continuum of positive energies corresponding to "free" states [24]. As soon as an arbitrarily weak field F is switched on, the continuum spectrum extends over the whole real axis, and the ground state is transformed into a decaying resonant state (Fig. 1). There is also an infinite set of short-lived resonances (metastable states) which correspond to the quasilocalized wave packets temporarily trapped between the classically forbidden territory (due to the external field potential) and the binding Dirac-δ potential. These resemble the Fabry–Perot resonances in that their complex energies are approximately equidistant with positive real parts. These states, indicated as "family one" in Fig. 1,

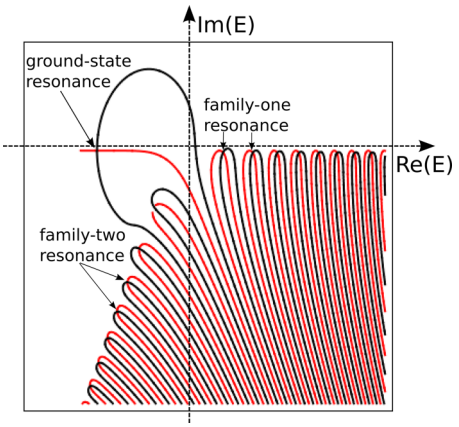

FIG. 1. (Color online) Resonance states in Dirac-δ system. Two staggered sets of curves (red and black online) show the respective zero-contours of the real and imaginary parts of the resonance-eigenvalue equation, with the intersections showing the locations of complex resonance energies. States with energies close to the positive real axis (family one) are those in which the system can retain some information about its history.

correspond to positive energies which would not be bound in the absence of the external field. However, their wave packets spend enough time in the vicinity of the atom potential, so they can "remember" the history of excitation. Note that the quantum-particle current due to the external field is completely classical in the absence of the atomic potential. Consequently, electronic states must be able to survive close to the ion in order to exhibit any dependence on the history of the excitation.

There exists yet another family of resonances (indicated as "family two" in Fig. 1) corresponding, roughly speaking, to the negative continuum energies (in the field). These states are coupled to the ground-state resonance because of the time dependence of the external field but have exceedingly short lifetimes. As such they act to renormalize the decay rate of the resonant ground state.

This model has been studied also in other contexts (see, e.g., Refs. [25,26] and references therein). Here we take the advantage of the fact that an exact solution for the induced dipole moment and current has been obtained for an arbitrary time-dependent field $F(t)$ [19], and the survival probability of the ground state can be calculated exactly. The observable most suited for the present purposes is the value of the wave function at $\psi(z=0,t)$, i.e., at the point where it "overlaps" with the contact potential. The reason we utilize this particular quantity is twofold. First, its value for times after the driving pulse has passed represents the population of the ground state. Second, its temporal evolution during the pulse reveals high-frequency oscillations due to the resonant states which mediate the effects we aim to study.

Besides the certainty that comes with an exact solution, the rationale behind using this Dirac-δ atom model is that it allows us to demonstrate that the existence of bound states is not a necessary condition for the occurrence of quantum history-dependent effects. Indeed, this system has no other bound states other than the ground state, yet the short-lived resonances turn out to be sufficiently stable to cause the

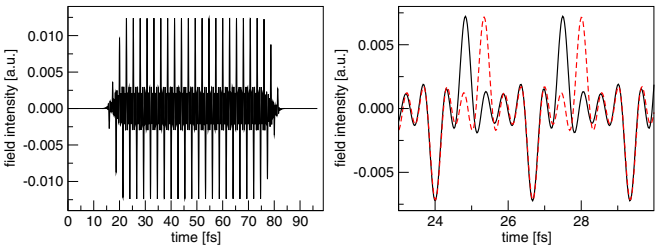

FIG. 2. (Color online) Synthesized subcycle pulse trains. The left panel shows the intensity versus time (in femtoseconds). Only pulse train A is shown because, at this scale, waveform B looks the same. The right panel shows two fundamental periods in both pulse streams. Note that the strong unipolar impulses are the same in amplitude and only differ in their relative timing.

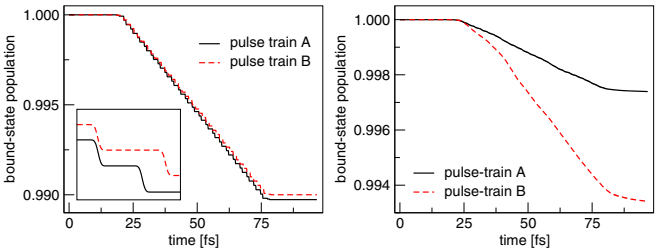

FIG. 3. (Color online) Survival probability (nonionization) of a model atom as calculated by the rate-ionization model (left panel) and according to the TDSE (right panel). The effective multiphoton order for the rate model is $K = 6.5$ and the ionization cross section is chosen such that the final ionization probability in pulse train A is 1%. The fundamental excitation wavelength is $\lambda = 800$ nm. The inset in the left panel shows a detail of the bound-state population vs time and illustrates that most of the ionization occurs during the strong electric-field impulses. These "steps" are smoothed out in the TDSE measurement due to the size of the computational domain.

dependence of the effective ionization rate on the history of the system.

Excitation with synthesized waveforms. To construct pulsed waveforms with attosecond-scale temporal features, we superimpose multiple harmonics as in Ref. [11], resulting in a δ-like train of peaks that are achieved by adding all harmonics in phase and with equal amplitudes. A similar pulse train, but with opposite sign of the electric field, is then generated and delayed with respect to the first. Figure 2 shows waveform A (left panel and red-dashed line in right panel) obtained by choosing the delay $\tau_d = 0.5T$ (with T being the period of the fundamental cycle), such that the high-intensity pulses of opposite polarity are equidistantly spaced in time and waveform B (black-solid line in right panel), with $\tau_d = 0.3T$, which results in a pattern of strong-intensity pulses of opposite sign that hit as a fast double pulse, after which a longer period of relatively low intensity follows.

These specific delays are chosen because they (and only they) produce extremely similar high-intensity portions of these wave trains, which is crucial for our demonstration. In simulations of femtosecond filaments, ionization is caused essentially solely by the highest-intensity portions of an optical pulse, whether it is implemented as a function of $E(t)$ or $I(t)$. Any ionization model that neglects the history of the system will predict that these two waveforms yield essentially identical ionization rates. This is demonstrated in Fig. 3 (left) which shows the survival probability of an atom described by the femtosecond filamentation ionization model. The small deviation is to be attributed to the differences of the relatively weak "backgrounds" in the two driving waveforms.

Because for a spatially and temporally resolved pulse-propagation simulation there has not been a practically applicable ionization model which could account for how the yield may depend on history, essentially all such computer-aided investigations would predict the same yield for these waveforms.

Next we examine how this behavior changes when the full quantum dynamics is accounted for in the TDSE-simulated model atom. We examined a range of intensities and wavelengths and found that history-dependent effects exhibit a strong influence on the effective ionization rate, as summarized in the following.

The right panel of Fig. 3 shows the comparison of the survival probability of the atom when it is exposed to the waveforms A or B derived from the fundamental wavelength $\lambda = 800$ nm. We find that the total ionization displays a remarkable difference, with waveform A roughly three times stronger than waveform B. This is clear evidence that, when shaping waveforms at the subfemtosecond scale, nontrivial light-matter interaction dynamics will occur that are not captured by the "stationary" ionization rates.

We may expect that the history-dependent effects must disappear at sufficiently slow driving, as one should then enter a fully adiabatic regime. The onset of this behavior can indeed be observed in Fig. 4. The left panel is obtained for $\lambda = 1200$ nm. Here, the difference in the ionization rates becomes smaller, although it is still very pronounced. Interestingly, it is now waveform B that is causing stronger ionization. This behavior is likely due to a resonance, possibly in conjunction with Stark-effect-induced shifts in the spectrum of the system. Which waveform is more ionizing is not only system specific, but also may depend on the intensity of the driving field, and we have not found a way to intuit or "predict" the outcome in any given case.

Finally, at the even longer wavelength $\lambda = 2400$ nm, the right panel of Fig. 4 shows that dependence on the system history becomes negligible, and the ionization is essentially the same in both waveforms. As expected for this long

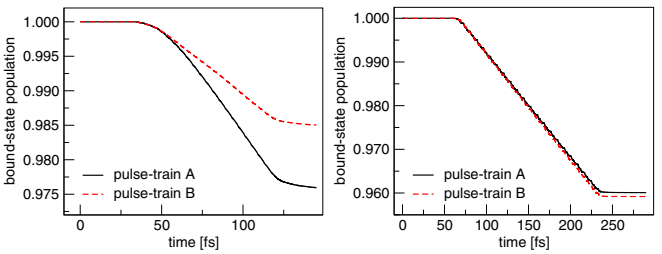

FIG. 4. (Color online) Ionization in synthesized pulse trains for fundamental harmonic wavelengths $\lambda = 1200$ nm (left panel) and $\lambda = 2400$ nm (right panel).

wavelength we have entered the adiabatic regime, in which the system follows the instantaneous value of the driving field and the relative timing between unipolar impulses is therefore unimportant. The transition into the adiabatic regime occurs similarly for the exactly solvable Dirac-δ system. In that case it is also possible to show analytically that nonadiabatic corrections scale with $1/\lambda^2$.

We have thus seen that the ionization-efficiency *differences* depend on the fundamental wavelength and thus on the spectral content of the electric field waveform. The fact that the two types of excitation can result in larger or smaller ionization rates at different wavelengths suggests that resonances mediated by the bound states of the atom affect the outcome. One could thus assume that the existence of multiple bound states is a necessary condition to observe the history effect in the ionization. However, as we demonstrate in the following, it turns out that the mere existence of a single bound state (e.g., the ground state) in conjunction with the energetic continuum is sufficient for the coherent history-dependent effects to set in as soon as the driving waveform is sufficiently "fast."

In order to show this, we employ the exactly solvable Dirac-δ atom model described above to investigate waveform timing effects in ionization and dynamics of the driven quantum system. Figure 5 shows the behavior of the wave-function amplitude $\psi(x=0,t)$ when the system is exposed to the same pulse trains we used above for the more realistic atom model. Its final value after excitation ceases is a direct measure of the nonionization survival probability. Comparison of the two panels reveals that the ionization yield is drastically dependent on the timing of the electric-field pulses. In other words, the system's response depends on its own history, as it makes a difference whether an equivalent electric-field impulse follows quickly after a previous one. This effect is further illustrated in Fig. 6, which shows a zoom into Fig. 5. A feature to note is the different amplitude of the wave-function oscillation immediately following the second field impulse. Reference [27] showed that, in the adiabatic approximation, it is exactly the amplitude of the metastable state (or Siegert resonance)

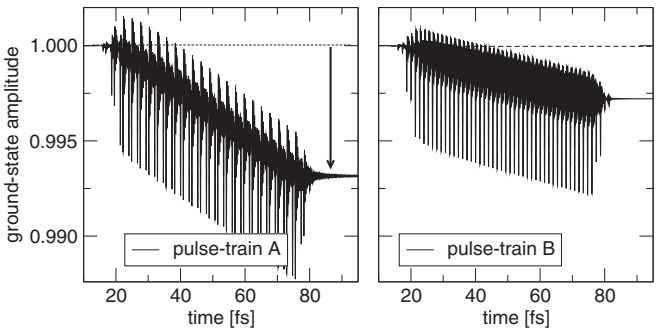

FIG. 5. Exactly solvable one-dimensional atom model exposed to a multicolor time-dependent driving field. The ground-state amplitude $\psi(x=0,t)$ is shown as a function of time. It exhibits adiabatic following of the driving field (large-scale variations) together with high-frequency oscillations due to interference between the ground and continuum states (causing, in particular, excursion exceeding unity). The final value after excitation reflects ionization (indicated by arrow) and shows that different pulse timings result in different effective ionization rates.

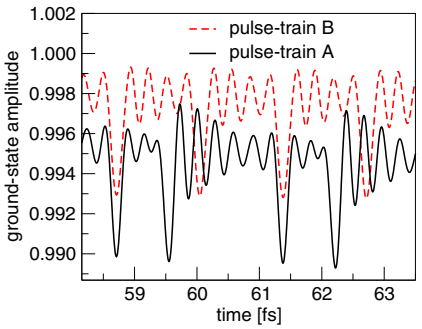

FIG. 6. (Color online) Resonance excitation as seen in a zoom-in on the same data as shown in the previous figure. Plots illustrate "shaking" of the electronic wave function in the external field. Note the increased amplitude of oscillation after the second impulse in pulse train A. These oscillations are due to excitation of low-lying resonance states labeled "family one" in Fig. 1.

born from the ground state that describes the wave function of the system, and in particular $\psi(x=0,t)$. The latter, when calculated in such an approximation, shows a smooth curve slaved to the optical field and has no dependence on the history. This tells us that what we see is the interference between the ground-state amplitude and the family-one resonant states shown in Fig. 1. The stronger "ringing" caused by the waveform A suggests that the increase in the ionization yield is mediated by these resonant states.

Conclusion. In conclusion, we have shown that, in the nonadiabatic regime, the atom dynamics, and in particular ionization yields, are strongly influenced by "field-dressed, weakly bound states," i.e., electronic states that survive in the vicinity of the atom or molecule for some time, even if only for a fraction of the optical cycle and are thus exposed to both the atomic potential and to the driving field. These dynamically driven superpositions are able to record the history of the system and exhibit a strong response even to weak fields. History-dependent effects may therefore occur even at low, readily achievable intensities and in driving waveforms with all frequencies much lower than the ionization potential, with possible applications in molecular fragmentation dynamics [28] and in the general field of extreme nonlinear optics.

One could ask what kind of excitation makes the system to "remember" its past. Unfortunately, the degree of nonadiabaticity in multicolor waveforms is not obvious. The Keldysh parameter of each individual frequency component in our wave trains indicates the multiphoton regime. On the other hand, constructively enhanced field strength combined with the slowest timescale results in a Keldysh parameter an order of magnitude smaller. This leads us to speculate that the pulses that enhance the dependence on the history should posses more than one characteristic field-strength and multiple timescales.

Last but not least, ionization by shaped wave trains presented in this work presents an ideal test scenario for approximate models of strong-field ionization models which could be applicable in spatially resolved intense-pulse simulations. Numerically exact methods, such as time-domain Schrödinger equation solutions, can be utilized to obtain ionization yields

for the proposed special class of wave trains in a range of field strengths and for various fundamental wavelengths. While it is to be expected that history-dependent effects occur in general multicolor pulses, the waveforms used in this paper enhance their "visibility" by maximizing the ionization-yield difference through a particular choice of relative timing. Only a model that correctly captures the difference between ionization yields as observed here can be trusted in truly multicolor or extremely broadband fields. To the best of our knowledge such models are yet to be developed.

Acknowledgments. This work was supported by the United States Air Force Office of Scientific Research (AFOSR) under Grants No. FA9550-13-1-0228 and No. FA9550-10-1-0561. D.F. acknowledges financial support from the European Union Seventh Framework Programme (FP/2007-2013) / ERC Grant Agreement No. 306559.

[1] K. Zhao, Q. Zhang, M. Chini, Y. Wu, X. Wang, and Z. Chang, Opt. Lett. **37**, 3891 (2012).
[2] A. N. Pfeiffer, C. Cirelli, M. Smolarski, R. Dörner, and U. Keller, Nat. Phys. **7**, 428 (2011).
[3] M. Uiberacker *et al.*, Nature (London) **446**, 627 (2007).
[4] A. N. Pfeiffer, C. Cirelli, M. Smolarski, D. Dimitrovski, M. Abu-samha, L. B. Madsen, and U. Keller, Nat. Phys. **8**, 76 (2012).
[5] M. Fieß *et al.*, New J. Phys. **13**, 033031 (2011).
[6] E. Goulielmakis *et al.*, Nature (London) **466**, 739 (2010).
[7] M. Gertsvolf, M. Spanner, D. M. Rayner, and P. B. Corkum, J. Phys. B: At., Mol. Opt. Phys. **43**, 131002 (2010).
[8] A. Schiffrin *et al.*, Nature (London) **493**, 70 (2013); M. Schultze *et al.*, *ibid.* **493**, 75 (2013).
[9] D. D. Yavuz, D. R. Walker, M. Y. Shverdin, G. Y. Yin, and S. E. Harris, Phys. Rev. Lett. **91**, 233602 (2003).
[10] W.-J. Chen *et al.*, Phys. Rev. Lett. **100**, 163906 (2008).
[11] H.-S. Chan *et al.*, Science **331**, 1165 (2011).
[12] H.-S. Chan *et al.*, Opt. Lett. **37**, 2805 (2012).
[13] W.-J. Chen, H.-Z. Wang, R.-Y. Lin, C.-K. Lee, and C.-L. Pan, Laser Phys. Lett. **9**, 212 (2012).
[14] S.-W. Huang, G. Cirmi, J. Moses, K.-H. Hong, S. Bhardwaj, J. R. Birge, L.-J. Chen, E. Li, B. J. Eggleton, G. Cerullo, and F. X. Kärtner, Nat. Photonics **5**, 475 (2011).
[15] P. Wei, J. Miao, Z. Zeng, C. Li, X. Ge, R. Li, and Z. Xu, Phys. Rev. Lett. **110**, 233903 (2013).
[16] L. V. Keldysh, Sov. Phys. JETP **20**, 1307 (1965).
[17] A. M. Perelomov, V. S. Popov, and M. V. Terentév, Sov. Phys. JETP **23**, 924 (1966).
[18] A. M. Perelomov, V. S. Popov, and M. V. Terentév, Sov. Phys. JETP **24**, 207 (1967).
[19] J. M. Brown, A. Lotti, A. Teleki, and M. Kolesik, Phys. Rev. A **84**, 063424 (2011).
[20] Y. Xiang, Y. Niu, and S. Gong, Phys. Rev. A **80**, 023423 (2009).
[21] V. Prasad, B. Dahiya, and K. Yamashita, Phys. Scr. **82**, 055302 (2010).
[22] J. Kasparian, R. Sauerbrey, and S. L. Chin, Appl. Phys. B: Lasers Opt. **71**, 877 (2000).
[23] E. Lorin, S. Chelkowski, and A. Bandrauk, Phys. D **241**, 1059 (2012).
[24] A. Teleki, E. M. Wright, and M. Kolesik, Phys. Rev. A **82**, 065801 (2010).
[25] J. M. Brown, E. M. Wright, J. V. Moloney, and M. Kolesik, Opt. Lett. **37**, 1604 (2012).
[26] M. Kolesik, E. M. Wright, J. Andreasen, D. Carlson, and J. R. Jones, Opt. Express **20**, 16113 (2012).
[27] O. I. Tolstikhin, T. Morishita, and S. Watanabe, Phys. Rev. A **81**, 033415 (2010).
[28] X. Xie, S. Roither, M. Schöffler, E. Lötstedt, D. Kartashov, L. Zhang, G. G. Paulus, A. Iwasaki, A. Baltuška, K. Yamanouchi, and M. Kitzler, Phys. Rev. X **4**, 021005 (2014).